REPORT DOCUMENTATION PAGE

Form Approved
OMB No. 0704-0188

1. REPORT DATE *(DD-MM-YYYY)*
06-06-2006

REPRINT

4. TITLE AND SUBTITLE
Observational Properties of Coronal Mass Ejections

5a. CONTRACT NUMBER

5b. GRANT NUMBER

5c. PROGRAM ELEMENT NUMBER
61102F

6. AUTHOR(S)
Kahler, S.W.

5d. PROJECT NUMBER
2311

5e. TASK NUMBER
RD

5f. WORK UNIT NUMBER
A1

7. PERFORMING ORGANIZATION NAME(S) AND ADDRESS(ES)
Air Force Research Laboratory/VSBXS
29 Randolph Road
Hanscom AFB MA 01731-3010

8. PERFORMING ORGANIZATION REPORT NUMBER
AFRL-VS-HA-TR-2007-1047

9. SPONSORING / MONITORING AGENCY NAME(S) AND ADDRESS(ES)

10. SPONSOR/MONITOR'S ACRONYM(S)
AFRL/VSBXS

11. SPONSOR/MONITOR'S REPORT NUMBER(S)

12. DISTRIBUTION / AVAILABILITY STATEMENT
Approved for Public Release; Distribution Unlimited.

13. SUPPLEMENTARY NOTES
REPRINTED FROM: SOLAR ERUPTIONS AND ENERGETIC PARTICLES, Geophysical Monograph Series 165, American Geophysical Union, 10.1029/165GM05, 2006.

14. ABSTRACT

Coronal mass ejections (CMEs) have been known and observed for over 30 years. The total number of observed CMEs is now approaching 10,000, most of them detected with the LASCO coronagraph on the SOHO spacecraft. We review statistical work on CME widths, latitudes, accelerations, speeds, masses, and rates of occurrence. Solar-cycle variations of these parameters are presented. Recent work has focused on CME internal properties and compositions and on CME dynamics, particularly at low (< 3 $R_\odot$) altitudes. The challenges to understand the magnetic topology of narrow (< 20° width) CMEs, to determine the relationship of coronal holes to CMEs, and to observe magnetic reconnection that effects magnetic disconnections of CMEs from the Sun are discussed.

15. SUBJECT TERMS
Sun Corona Coronal Mass Ejections Particle emission

16. SECURITY CLASSIFICATION OF:			**17. LIMITATION OF ABSTRACT**	**18. NUMBER OF PAGES**	**19a. NAME OF RESPONSIBLE PERSON**
a. REPORT		**c. THIS PAGE**			S. W. Kahler
UNCLAS	UNCLAS	UNCLAS	SAR	10	**19b. TELEPHONE NUMBER** *(include area code)* 781-377-9665

Observational Properties of Coronal Mass Ejections

S.W. Kahler

Air Force Research Laboratory, Space Vehicles Directorate, Hanscom AFB, Massachusetts

Coronal mass ejections (CMEs) have been known and observed for over 30 years. The total number of observed CMEs is now approaching 10,000, most of them detected with the LASCO coronagraph on the SOHO spacecraft. We review statistical work on CME widths, latitudes, accelerations, speeds, masses, and rates of occurrence. Solar-cycle variations of these parameters are presented. Recent work has focused on CME internal properties and compositions and on CME dynamics, particularly at low (< 3 $R_\odot$) altitudes. The challenges to understand the magnetic topology of narrow (< 20° width) CMEs, to determine the relationship of coronal holes to CMEs, and to observe magnetic reconnection that effects magnetic disconnections of CMEs from the Sun are discussed.

1. INTRODUCTION

Coronal mass ejections (CMEs) have now been observed for over three decades. The earlier observations from the OSO-7, Skylab, Solar Maximum Mission (SMM), and Solwind coronagraphs have been reviewed and compared with the current coronagraph observations from the LASCO coronagraphs on SOHO by *Gopalswamy et al.* [2003] and *Yashiro et al.* [2004], who emphasized the LASCO CME annual variations, and by *Gopalswamy* [2004], who emphasized the mission-cumulative statistics. Here we briefly review the statistical properties of CMEs presented in those works using the large database of ~7000 LASCO CMEs, whose parameters are measured from sequences of running difference images and are given in the web-based catalog of CMEs provided by the Catholic University of America (CUA) [*Yashiro et al.*, 2004]. *Robbrecht and Berghmans* [2004 and this volume] discuss an automated CME recognition program to provide an objective and more comprehensive method of selecting and measuring CMEs.

The CME images are projections on the plane of the sky, so some measured properties such as CME speeds and masses can be only lower limits and others such as CME widths and latitudes only upper limits, rather than true values [*Burkepile et al.*, 2004]. For each CME the speed of only the fastest part of the leading edge is measured with both first and second order fits. Angular widths around the coronagraph occulting disk and position angles (PA) measured counterclockwise from north are also given. Halo CMEs (Figure 1) are defined as CMEs with angular widths ≥ 120° and are treated separately. Masses of LASCO CMEs have only recently been compiled statistically and are reviewed. The CME statistics from solar minimum in 1996 through the recent maximum in 2000 have allowed us to compare the CME properties of the two extreme periods of solar activity.

We also review recent work on more detailed observations to describe the early dynamics and structures of CMEs and then discuss three research topics that appear ripe for new advances. These are the magnetic topologies of narrow (< 20°) CMEs; coronal magnetic reconnection in CMEs; and the relationship of coronal holes (CHs) to CMEs.

2. CME STATISTICS

2.1. Occurrence Rates of CMEs

The CME occurrence rate is an index of solar activity. It has long been known to track the sunspot number and other indices of solar activity. Figure 2 [*Gopalswamy*, 2004] compares the smoothed LASCO CME rate with the sunspot number, showing good agreement, although with some lag

Solar Eruptions and Energetic Particles
Geophysical Monograph Series 165

10.1029/165GM05

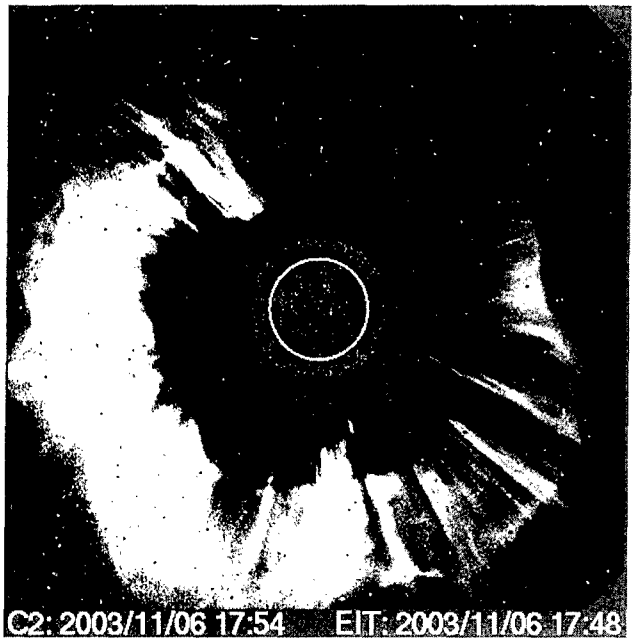

Figure 1. A LASCO 360° halo CME of 6 November 2003 shown as a subtracted image. The CUA website gives a speed of 1523 km s^{-1} measured at a PA of 100° and an acceleration of −59.5 m s^{-2}. The white circle is the solar disk, and the C2 coronagraph inner limit of the field of view lies at 2.2 $R_\odot$ The dark circular band is caused by subtracting the previous LASCO image taken 24 minutes earlier.

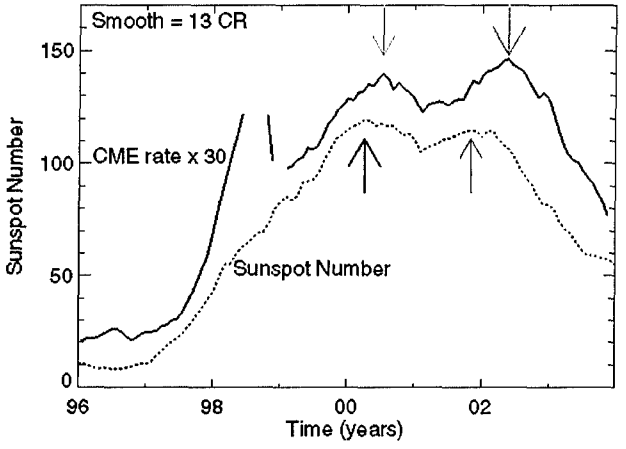

Figure 2. The LASCO CME rate smoothed over 13 Carrington rotations and compared with the solar sunspot number. Arrows indicate the two maxima in CME rate and sunspot number. Large data gaps occurred during June 1998 to February 1999. From *Gopalswamy* [2004].

near the two sunspot number peaks. The lag is probably related to the fact that high latitude (> 60°) CMEs, arising in the polar crown filaments, are also important near solar maximum but are not directly related to the sunspot number [*Gopalswamy et al.*, 2003]. The low-latitude CME rate increased in a step-like fashion in 1998 and remained relatively constant while the high latitude CME rate was much more variable. The CME occurrence rate is less than 1 CME/day at solar minimum and about 6 CME/day at solar maximum.

2.2. Latitudes of CMEs

CMEs tend to be confined to low-latitude streamer belts at solar minimum and to range over a broad latitude range at solar maximum. *Yashiro et al.* [2004] have compiled the annual solar latitude distributions of the LASCO CME PAs from 1996 at solar minimum through 2002. The solar latitude ranges that contain 80% of the CME PAs for those years range from (~22°) in 1996 to (~63°) at maximum in 2000. Halo CMEs were not included in the statistics.

2.3. Widths of CMEs

Angular widths of all LASCO CMEs observed from 1996 through August 2003 have been compiled by *Gopalswamy* [2004]; the average width of all non-halo (width ≤ 120°) CMEs is 47° (Figure 3). It is convenient to divide CMEs into three width groups: narrow (< 20°), normal (20° to 120°) and wide, or halos, (≥ 120°). *Yashiro et al.* [2004] found that over the years 1996-2002 the three width groups were distributed as: narrow, 18%; normal, 70%; and halo, 12%. There was an increase in the median widths of normal CMEs from 43° at the 1996 solar minimum to 58° in 1999 and then a decrease to 49° in 2002. During the period 1998-2000 a bimodal distribution appeared, with peaks at ~15° and ~50°. The average widths do not appear to vary with latitude [*Michalek and Mazur*, 2002].

CME angular widths may vary with height. *St. Cyr et al.* [1999] compared the widths of 132 CMEs observed in both the 1.15 to 2.4 $R_\odot$ and the 1.7 to 6 $R_\odot$ fields of view of the Mark III coronameter and the SMM coronagraph, respectively. They found an average 12° increase in the SMM widths, which they interpreted as a 20% to 30% increase in angular span as the CMEs traveled from the inner to the middle corona. However, *Stockton-Chalk* [2002] found only a modest average nonradial expansion of 1.84°, corresponding to a width increase of 3.7°, in 50 CMEs measured at various points in the ~5 to 25 $R_\odot$ range of the LASCO C2 field of view.

Inclusion of adjacent pre-existing streamer deflections or wave-like coronal disturbances as parts of the CMEs can result in over-estimations of intrinsic CME widths [*Cremades and Bothmer*, 2004], particularly for halo CMEs [*Michalek et al.*, 2003; *St. Cyr et al.*, 2005; Sec. 2.6]. In those cases the smaller widths measured when the CME leading edges are still in the LASCO C2 field of view may provide more

realistic CME widths. In their study of structured CMEs [Sec. 3.2] *Cremades and Bothmer* [2004] found an average width of 85°, much smaller than the 155° value derived from the same CME widths of the CUA catalog.

2.4. Speeds and Accelerations of CMEs

The CME linear-speed distribution through 2003 is shown in Figure 3, where the average value of 489 km s^{-1} is indicated [*Gopalswamy*, 2004]. Only 25 of the 7567 CME speeds exceeded 2000 km s^{-1}; the fastest CME speed measured thus far was 2657 km s^{-1} on 4 November 2000. When compiled on an annual basis, there is a very clear increase in average annual speeds from 281 km s^{-1} in 1996 to 560 km s^{-1} in 2003. CME speeds as a function of width declined slightly over the range 0° to ~65° and then increased with considerable scatter over larger widths [*Yashiro et al.*, 2004].

CME accelerations are important for the insights they can provide into the balance among the Lorentz, gravitational, and drag forces [*Vršnak et al.*, 2004]. When 5 or more data points were available in the LASCO height-time plots, second-order fits could be done to obtain accelerations. The results showed an anticorrelation between acceleration and speed in that slower CMEs generally accelerated and faster CMEs decelerated [*Yashiro et al.*, 2004; *Gopalswamy*, 2004], a result attributed to aerodynamic drag [*Vršnak et al.*, 2004]. The average deceleration of the fastest (> 900 km s^{-1}) CME group is −16 m s^{-2}, comparable to that of solar gravity at 5 $R_\odot$ (−11 m s^{-2}). The accelerations decline for CMEs with larger widths and at greater solar distances such that CMEs are nearly at solar wind speeds within the 30 $R_\odot$ LASCO field of view. However, a small (≤ 10% fraction of CMEs, generally broader and faster than the rest of the CME sample, continue to be propelled beyond 25 $R_\odot$ [*Vršnak et al.*, 2004].

2.5. Masses and Energies of CMEs

The most recent distribution of LASCO CME masses includes 4297 CMEs observed through the end of 2002 and with widths between 10° and 150°. The average and median values for those CMEs are 1.57×10^{15} gms and 6.67×10^{14} gms, respectively [*Vourlidas*, 2004)]. We compare the LASCO mass distribution with those from the Solwind [*Jackson and Webb*, 1994] and SMM [*Burkepile et al.*, 2004] coronagraphs in Figure 4. The earlier measurements were more characteristic of solar maximum, and the characteristic values are higher. However, the ~15% of CMEs with masses below 10^{14} gms appears to be the result of the higher LASCO sensitivity [*Vourlidas et al.*, 2002]. *Vourlidas et al.* [2002] found a positive correlation between CME masses and accelerations, i.e., small mass CMEs tended to decelerate while the large-mass CMEs accelerated.

The CME kinetic energies can also be calculated from the LASCO measured masses and speeds. The average (median)

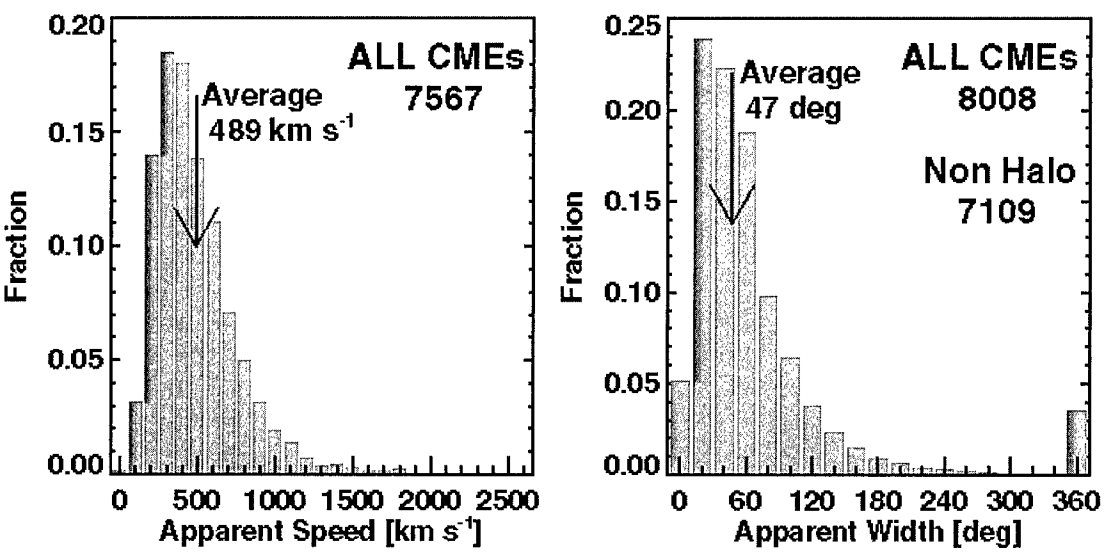

Figure 3. Distributions of LASCO CME speeds (left) and widths (right) from 1996 through 2003; the arrows indicate distribution averages. Apparent speeds are measured in the plane of the sky at the PA of the fastest moving part of the CME leading edge. Speeds could be measured for only 7567 of the total 8008 detected CMEs. The average width of 47° corresponds only to the 7109 nonhalo (≤ 120°) CMEs. From *Gopalswamy* [2004].

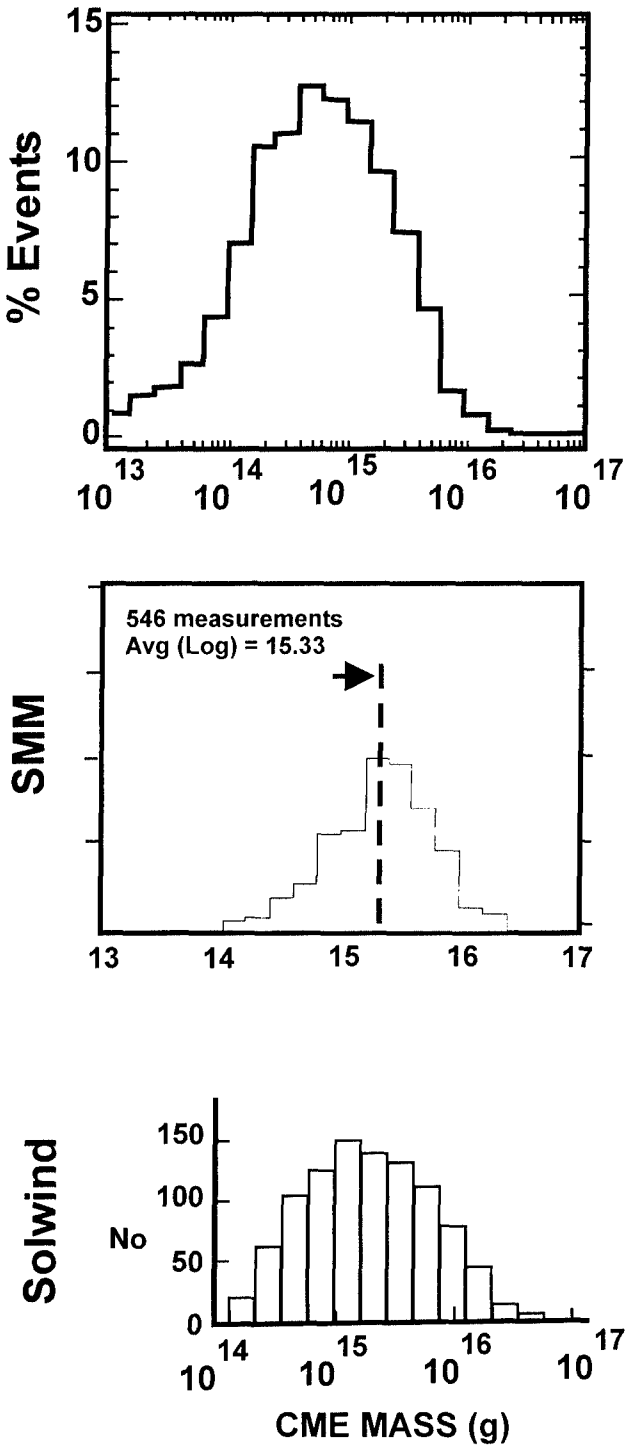

Figure 4. CME mass distributions from LASCO (top), SMM (middle), and Solwind (bottom). The mass scales in logs of masses in grams are approximately aligned for all plots. From *Vourlidas* [2004], *Burkepile et al.* [2004], and *Jackson and Webb* [1994].

kinetic energy is 2.4×10^{30} ergs (5.0×10^{29} ergs) [*Vourlidas*, 2004].

2.6. Halo CMEs

Halo CMEs (Figure 1) can be full (360°) or partial (> 120°). Based on a study of the widths of SMM limb CMEs *Burkepile et al.* [2004] concluded that halo CMEs are typical CMEs originating close to disk center and directed preferentially along the Sun-Earth line, either toward or away from the Earth. However, the average speed of LASCO halo CMEs during 1996-2003 was 1004 km s^{-1}, well above the average speed of 489 km s^{-1} for the general CME population [*Gopalswamy*, 2004]. Those directed toward the Earth are often associated with shocks, solar energetic particle (SEP) events, and geomagnetic storms and therefore merit consideration as a more energetic group of CMEs [*Michalek et al.*, 2003; *Gopalswamy*, 2004], contrary to the conclusion of *Burkepile et al.* [2004]. Three different types of halo CME are now recognized [*St. Cyr et al.*, 2005]: 1. eruptions lying near the Sun-Earth line; 2. eruptions causing deflections of pre-existing coronal structures; and 3. the coalescence of multiple CMEs. Those of the second type can lie near the limb. All types are illustrated at the CUA LASCO website.

Full halos are ~3.5% [*Gopalswamy*, 2004] and partial halos (> 120°) are ~12% [*Yashiro et al.*, 2004] of all CMEs. Most full halo CMEs are faster than 900 km s^{-1} and therefore a subset of a group of fast (> 900 km s^{-1}) and wide (> 60°) CMEs, which are particularly efficient in driving shocks [*Gopalswamy*, 2004] and producing SEPs [*Kahler and Reames*, 2003]. The fast-and-wide CMEs constitute about 4.7% of the total CME population and generally track the total CME population in occurrence rate.

2.7. Solar Cycle Variations of CMEs

We summarize the solar-cycle variations of CME characteristics in Table 1. Those CME parameters generally increase from solar minimum in 1996 to solar maximum around 2001 as the contribution of CMEs to the solar wind and to space weather becomes more important around solar maximum.

3. CME EARLY DYNAMICS AND STRUCTURES

3.1. Early Dynamics of CMEs

Most of the acceleration of most CMEs occurs below the ~2.2 $R_\odot$ inner limit of the LASCO C2 coronagraph. The LASCO C1 coronagraph and other space or ground-based instruments have been used to understand the initial speed and acceleration profiles of CMEs. *St. Cyr et al.* [1999]

Table 1. Solar-Cycle Variations of CME Parameters

Parameter	Minimum	Maximum	Notes
Occurrence	< 1/day	~6/day	
Solar Latitude Range	22°	63°	Includes 80% of CMEs.
Median Widths[a]	43°	58°	1999 Maximum.
Average Widths[a]	47°	61°	1999 Maximum.
Median Speeds (km s^{-1})	250	495	2003 Maximum.
Average Speeds (km s^{-1})	281	560	2003 Maximum.
Accelerations	lower	higher	Not measured separately.
Masses	smaller	larger	Not measured separately.
Kinetic Energies	smaller	larger	Not measured separately.

[a] > 20° to ≤ 120° CMEs only.

combined ground-based MK3 and SMM CME observations to track 76 features in 55 CMEs above 1.15 $R_\odot$ Thirty features were consistent with a constant speed profile and 46 with a constant acceleration, the median value of which was 44 m s^{-2}. Those features associated with active regions were more likely to have constant speeds or, if accelerating, to have larger accelerations and to have higher final speeds than the features associated with prominence eruptions. On the basis of 4 flare-associated CMEs observed close to the limb in the LASCO C1 field of view (1.1-3 $R_\odot$) *Zhang et al.* [2001] found a three-phase kinematic profile. A slow rise (< 80 km s^{-1}) over tens of minutes constitutes the first phase; in the second phase a rapid acceleration of 100-500 m s^{-2} occurs in the height range ~1.4 to ~4.5 $R_\odot$ during the flare rise phase; the final phase is a propagation at a constant or declining speed. Subsequent detailed CME studies combining the LASCO C2 with other coronal observations [*Maričič et al.*, 2003; *Shanmugaraju et al.*, 2003; *Gallagher et al.*, 2003] have narrowed the strong (> 200 km s^{-1}) acceleration region of impulsive CMEs to ~1.5 to 3 $R_\odot$ However, *Zhang et al.* [2004] have shown that CMEs may not easily fall into the gradual/impulsive categories. Their three CMEs span a range from high speed with short and strong accelerations to low speed with long and weak accelerations.

A controversy about CME speeds began when *Sheeley et al.* [1999] distinguished two dynamical classes of CMEs: gradual CMEs, which are slower, accelerate in the coronagraph fields of view, and are preferentially associated with prominence eruptions; and impulsive (or fast) CMEs, which are faster, decelerate in the coronagraph fields of view, and are preferentially associated with solar flares. The two CME dynamical classes had been suggested earlier by *Gosling et al.* [1976] and *MacQueen and Fisher* [1983]. The basic question is whether there are two physically different processes that launch CMEs or whether all CMEs belong to a dynamical continuum with a single physical initiation process. Recent observational studies of CME and coronal flare/prominence associations and timings have claimed to support the two-class view [*Moon et al.*, 2002; *Zhang et al.*, 2002; *Zhang and Golub*, 2003]. Several cases of flare-associated CMEs with large accelerations in the range 5 to 15 $R_\odot$ were explained by *Moon et al.* [2004] in terms of effects of destabilization of helmet streamers and of subsequent flare/CME events rather than as evidence against two classes of CMEs. In addition, *Low and Zhang* [2002] have proposed a model of two kinds of CMEs originating from normal and inverse magnetic geometries in prominences. They found that CMEs arising in normal polarity eruptions have more energy and higher speeds, a result confirmed by numerical modeling [*Liu et al.*, 2003].

Evidence for a single dynamical CME class was presented by *Feynman and Ruzmaikin* [2004], who discussed a CME with a high (> 1500 km s^{-1}) speed, acceleration, and an erupting prominence association, thereby combining attributes of both dynamical types. In a recent comprehensive statistical analysis of 545 flare-associated and 104 non-flare CMEs *Vršnak et al.* [2005] found considerable overlap of accelerations and speeds between the two CME groups. While flare-associated CMEs are generally faster than those without flares, there is also a correlation between CME speeds and flare X-ray peak fluxes, in which CMEs associated with the small B and C class flares are similar to the CMEs associated with filament eruptions. Thus, they argue for a CME continuum and against the two-class concept.

Lin [2004] has discussed the two classes of CMEs based on a single catastrophe model for eruptions that treats the CME, flare, and prominence as constituents of a process that depends on the magnetic field intensity and structure and plasma density. Earlier, *Chen and Krall* [2003] found that their 3-D flux rope model could explain the observed distribution of CME accelerations in terms of one mechanism with two distinct phases of acceleration. A more compelling argument is based on the observational result that the speeds of both accelerating and decelerating LASCO CMEs are distributed lognormally [*Aoki et al.*, 2003; *Yurchyshyn et al.*, 2005], implying that the speeds of both groups result from many simultaneous processes or from sequential series of processes, as discussed by e.g., *Campbell* [2003] and *Bogdan et al.* [1988]. *Yurchyshyn et al.* [2005] interpret these processes as a multiple magnetic reconnection process; hence, there is no physical distinction between accelerating and decelerating CMEs. However, it is not obvious that a scheme of two CME acceleration classes, each of which

undergoes further coronal processes that modify their CME speeds, is precluded. The controversy is not yet settled, but the one-class continuum model should be regarded as preferred. CME initiation and numerical modeling are explored in detail in the reviews in this volume by *Moore and Sterling* and *Roussev*, respectively.

3.2. CME Structures

A large fraction of CMEs show a three-part structure consisting of a bright leading edge, a dark void, and a bright core [*Hundhausen*, 1999; *Gopalswamy*, 2004], as shown in the CME of Figure 5. The leading edge is compressed overlying coronal material; the void is assumed to originate in the prominence cavity and to be a magnetic flux rope; and the bright core corresponds to the erupting prominence. These features are readily distinguished in white light, but any analysis of the physical conditions within those structures, the prominence in particular, must be done with spectral observations. The SMM coronagraph included an Hα-band filter, which was used for studies of a few CMEs with large prominences. Comparisons of Hα and white light images from eight prominence/CMEs established that some CME prominence masses exceed 10^{15} gm, thus constituting a large fraction of total CME masses [*Illing and Athay*, 1986]. However, not all white-light prominences were enhanced in Hα. The evolution of the Hα brightness gradients in prominence features gives clues to the expansion and heating rates in those features [*Athay et al.*, 1987]. Comparison of ground-based Hα prominence observations with LASCO white light observations confirms that prominences can be followed into the C2 field of view, where they form the trailing edges of the coronal cavities of the CMEs [*Plunkett et al.*, 2000], and that their speeds are always less than the speeds of the white light leading edges [*Simnett*, 2000]. However, the leading edge and prominence accelerate simultaneously [*Maricic et al.*, 2004].

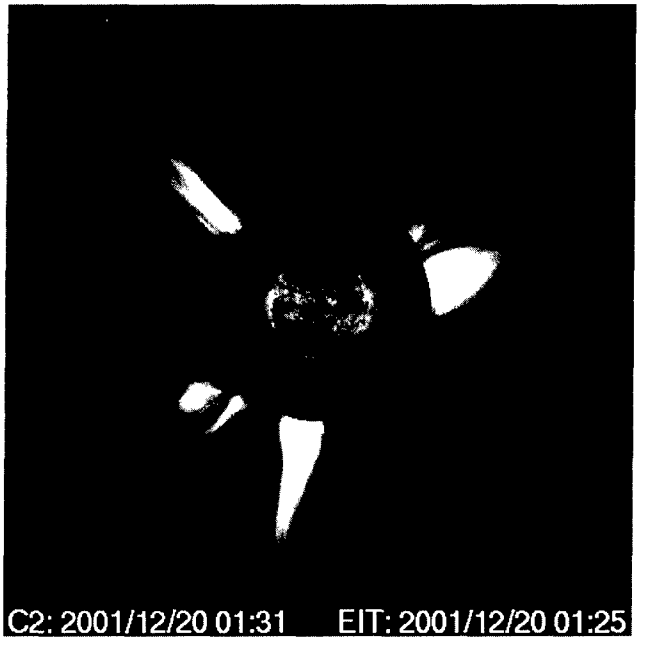

Figure 5. A LASCO CME over the southeast limb showing a three-part structure: a bright leading edge, a dark void, and a bright core. The inner image is the 195 *Å* solar disk image from the SOHO EIT.

Most coronagraph studies of CME structures are based on unpolarized, broad-band white light observations. However, CMEs have been observed with coronagraph polaroid [*Sheeley et al.*, 1980; *MacQueen et al.*, 1980; *Brueckner et al.*, 1995] filters. Coronagraph polaroid images can help to determine the average distances between CME masses and the plane of the sky. Because the polarization of CME Thomson-scattered light ranges from linear and tangential to the solar limb for CMEs that lie in the plane of the sky to unpolarized for CMEs lying near the Sun-Earth line, the ratios of polarized to unpolarized brightness can be used to construct topographic maps of the structures and positions of CMEs. The first detailed treatment of LASCO C2 polaroid CME observations [*Moran and Davila*, 2004] showed loop arcades and filamentary structure in two halo CMEs and one backside CME. A recent LASCO polaroid analysis [*Dere et al.*, 2005] of three CMEs in 2002 August also showed filamented loop arcade structures (Figure 6), one of which appeared to be a flux rope. Those results appear challenging for recent work to determine CME structure based on a simple cone model [*Zhao et al.*, 2002; *Xie et al.*, 2004] or CME evolution using a flux rope model [*Chané et al.*, 2005]. The review by *Nindos* in this volume explores the role of magnetic helicity in CMEs.

Cremades and Bothmer [2004] recently presented a simple scheme to relate CME structure to the heliographic position and orientation of the underlying magnetic neutral line. Working with a set of 124 LASCO CMEs showing intricate fine structure and for which relevant information about the CME source region could be determined, they found the following rule. When the neutral line is approximately parallel to the solar limb, the CME appears as a linear feature parallel to the limb and having a broad, diffuse inner core. When the neutral line is approximately perpendicular to the solar limb, the CME is observed along its symmetry axis, and the core material lies along the line of sight. Joy's law implies that the frontside neutral line lies predominately perpendicular to the east limb and parallel to the west limb, as indicated schematically in Figure 7. The neutral line and CME orientations are reversed for the solar backside, so the backside CMEs are viewed predominately orthogonally to frontside CMEs at each limb. These CME orientations are generally

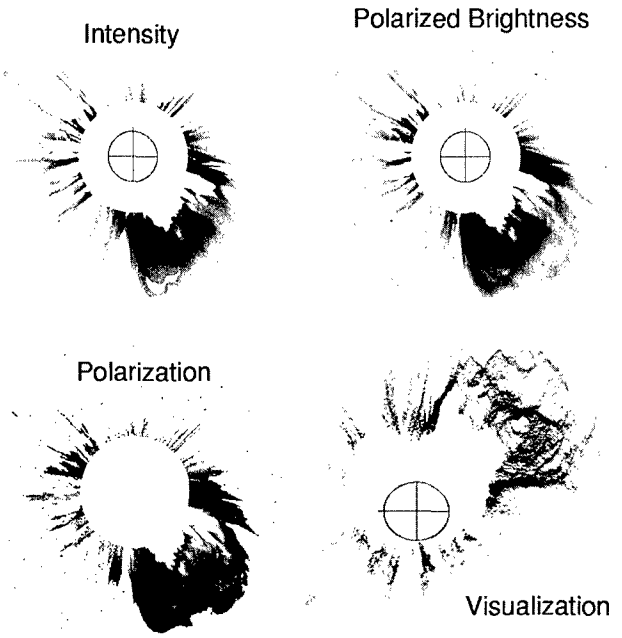

Figure 6. The intensity, polarized brightness, and polarization LASCO images of the CME of 7 August 2002 at 11:48 UT. The derived structure was rotated 90° counterclockwise in the sky plane and then tilted backwards by 30° along the new x axis for the visualization. The filamentary structure is common to other reconstructed CMEs. From *Dere et al.*, 2005.

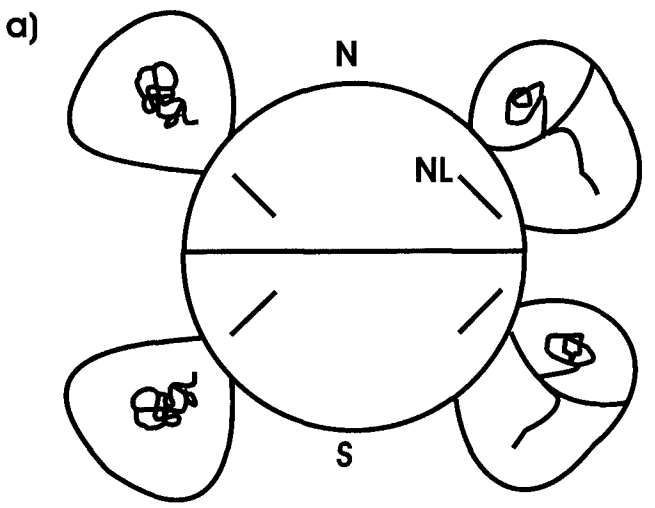

Figure 7. Schematic relating frontside neutral lines, oriented according to Joy's Law, to the envelopes of associated CMEs. CMEs on the east limb are observed along the symmetry axis; CMEs on the west limb perpendicular to the symmetry axis. The orientations reverse for backside neutral lines. From *Cremades and Bothmer* [2004].

valid only for CMEs with source regions in the active regions, below latitudes of ~50°. The CME orientations will be different for polar crown filaments [*McAllister et al.*, 2002; *Gopalswamy et al.*, 2003] or for CME source regions outside the active regions, where the neutral lines do not obey Joy's law.

The definition of a CME involves material in a magnetic field that is expelled from the corona [*Hundhausen*, 1999], so we assume that all the material observed in coronagraphs escapes the corona. However, in a few CMEs with relatively slow speeds material in bright cores collapses back to the Sun with speeds of ~50 to 200 km s^{-1} [*Wang and Sheeley*, 2002a]. These collapses have been interpreted in terms of gravitational and magnetic tension forces as well as the drag forces of the ambient solar wind. It is not clear whether these collapses are only a minor part of some CMEs or more generally important for the CME dynamics.

EUV spectral observations from the UVCS, CDS, and SUMER instruments on SOHO have defined CME densities, temperatures, ionization states, and Doppler velocities [*Raymond*, 2002]. Most CME material observed in UVCS is cool ($< 10^{55}$ K) and concentrated into small regions [*Akmal et al.*, 2001], although this is not the case for fast CMEs associated with X-class flares [*Raymond et al.*, 2003]. In one well observed case the prominence core reached coronal temperatures at the top and was cool at the base [*Ciaravella et al.*, 2003], in agreement with earlier SMM results [*Illing and Athay*, 1986]. In addition, heating rates inferred from models using UVCS observations show that heating of the material continues out to 3.5 $R_\odot$ and is comparable to the kinetic and gravitational potential energies gained by the CMEs [*Akmal et al.*, 2001]. The Doppler information from UVCS combined with the EIT and LASCO images has shown in one case the unwinding of a helical structure [*Ciaravella et al.*, 2000]. See the review by *Ciaravella and Raymond* in this volume for further discussion of spectroscopic investigations of CMEs and coronal shocks.

4. SELECTED QUESTIONS ABOUT CMES

4.1. Narrow CMEs

The possibility that narrow (5°-40°) CMEs are physically distinct from the general population of all CMEs was addressed by *Kahler et al.* [1989], who found that 22% of all impulsive > M1 X-ray flares were associated with Solwind CMEs. A common view [*Svestka*, 1986] was that all flares either are confined and not associated with CMEs or are CME-associated eruptive events. Since confined flares were presumed to be impulsive, the CME associations of some impulsive flares violated the basic confined-eruptive flare paradigm. A correlation between associated CME width

and X-ray flare duration implied [*Kahler et al.*, 1989] a single continuous class of CMEs rather than two CME classes, although the enhanced energetics and lack of postflare loop associations for impulsive flares with CMEs suggested a different kind of CME for the impulsive events.

The question of whether narrow CMEs are a physically distinct class of CMEs arose again when *Kahler et al.* [2001] reported an association of a narrow LASCO CME with an impulsive flare and SEP event on 1 May 2000 and found narrow CMEs associated with other impulsive SEP events. They drew on recent modeling work of *Shimojo and Shibata* [2000] to suggest that especially energetic coronal reconnection events can both accelerate particles and propel mass outward along open field lines as CMEs. The open magnetic-field topology of those CMEs would differ fundamentally from that of the larger, closed-field CMEs [*Reames*, 2002], and no magnetic flux would be expelled by the open-field CMEs. Figure 8 shows a cartoon of magnetic reconnection leading to the narrow CME along open field lines.

Gilbert et al. [2001] compared properties of 15 narrow (< 15°) CMEs with those of more typical CMEs to understand how the narrow CMEs were generated. The facts that their narrow CMEs were well associated with active prominences but not with surges led them to conclude that narrow CMEs originate in closed-field regions as do the larger CMEs. Models of properties of 5 of those narrow CMEs based on UVCS spectral observations were consistent with both reconnection jets on open fields and with closed-field CMEs [*Dobrzycka et al.*, 2003]. The speeds, widths, and flare and filament associations of the narrow CMEs of the *Gilbert et al.* [2001] study are very similar to those of the white-light coronal jets studied by *Wang and Sheeley* [2002b] during a comparable 1999 time period. The jets were associated with bipolar magnetic regions located near CH boundaries, similar to the good source associations of narrow CMEs with sharp bends in magnetic polarity-reversal lines [*Gilbert et al.*, 2001]. However, the jets were interpreted by *Wang and Sheeley* [2002b] in terms of reconnection between the CH open fields and bipolar magnetic-region closed fields with subsequent ejection of material along open field lines, contrary to the conclusion of *Gilbert et al.* [2001] regarding narrow CMEs.

Yashiro et al. [2003] surveyed the properties of narrow (< 20°) LASCO CMEs and found evidence for a bimodal distribution of CME widths during 1998-2000 as well as differences in speed distributions between normal and narrow CMEs. *Yashiro et al.* [2003] and *Wang and Sheeley* [2002b] argue that the jets are a separate population of narrow open-field CMEs; they deserve further study.

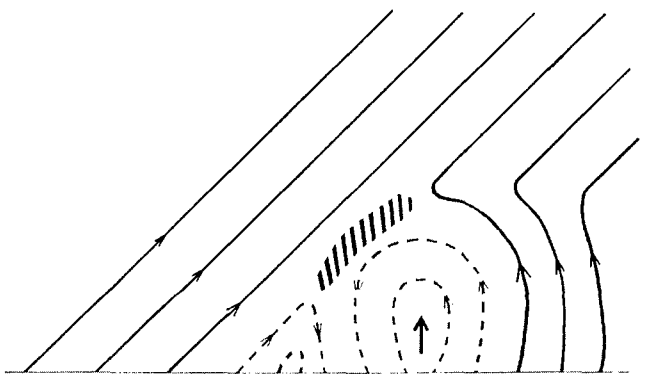

Figure 8. Schematic of magnetic reconnection between a closed-field region (dashed lines) and an overlying open-field region (solid lines). Reconnection occurs in the shaded region; mass on previously closed fields is ejected outward along open field lines. Adapted from *Reames* [2002] and *Shimojo and Shibata* [2000].

4.2. Reconnection in CMEs

The early realization that CMEs were continually injecting new magnetic flux into the interplanetary medium, although the magnetic flux there varies by less than a factor of 2 over the solar cycle [*Gosling*, 1975; *Wang and Sheeley*, 2002c], implied that magnetic reconnection must accompany or follow CMEs to detach the CME field lines from the Sun. Yohkoh Soft X-ray Telescope (SXT) observations have provided substantial X-ray evidence of post-CME reconnection, such as cusp-shaped loops [*Shibata*, 1999] and supra-arcade downflows [*McKenzie*, 2000] over long-duration flares. An extensive survey of post-eruptive arcades in SOHO 195 Å images has shown that every arcade is associated with a LASCO CME [*Tripathi et al.*, 2004]. These observations have been interpreted in terms of a basic model (named the CSHKP model to reflect its provenance) of reconnecting magnetic fields behind a magnetic flux rope and over a magnetic arcade (e.g., *Lin et al.*, 2004), which results in a disconnection of CME fields from the Sun, as shown in Figure 9. Correlations found between inferred magnetic reconnection rates in arcades and the speeds of associated CMEs provide further confirmation of the model [*Jing et al.*, 2005]. Radio imaging of the moving and quasi-stationary type IV bursts can provide upper limits to the current sheet length by bracketing the reconnection region [*Pick et al.*, 2005].

An observational challenge is to detect coronal white-light signatures of reconnection in the wakes of CMEs. *Webb and Cliver* [1995] looked in pre-LASCO coronagraphs for *Y*-shaped or concave-outward CME structures in which the vertical line of the *Y* is the reconnecting current sheet that

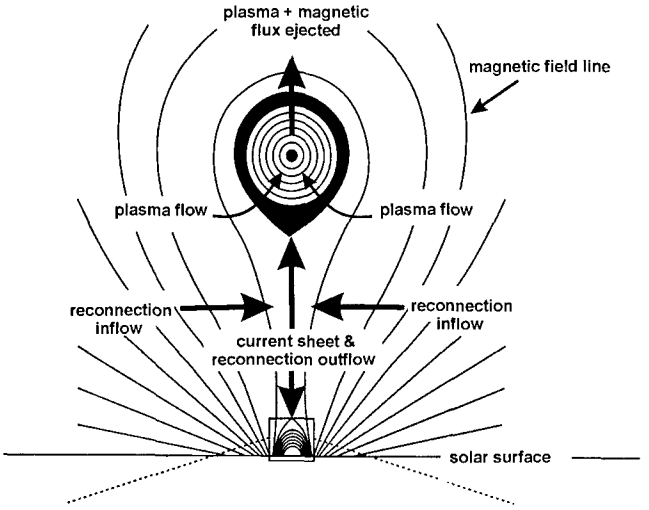

Figure 9. Basic CSHKP model of CMEs looking parallel to the magnetic neutral line. Solid lines are magnetic field lines. An inflow behind the ejected mass and magnetic flux produces the current sheet and post-eruptive arcade at bottom center, which forms a *Y*-shaped structure. Details of the flare and arcade are omitted here. Adapted from *Lin et al.* [2004].

appears as a bright ray (Figure 9). They concluded that > 10% of CMEs showed such structures. With the advent of LASCO, cases of *Y*-shaped CMEs were reported by *Simnett et al.* [1997], and *St. Cyr et al.* [2000] found such features in one third to one half of all LASCO CMEs. *Webb et al.* [2003] studied 26 SMM CMEs followed by narrow (~2.5°) rays extending to beyond 5 $R_\odot$ and concluded that they were consistent with two CME models predicting an extended long-lived current sheet. Bright narrow features with enhanced temperatures (3-6 × 10^6 K), densities (~5 × 10^7 cm^{-3} at 1.5 $R_\odot$) and abundances of elements with low first ionization potentials (FIPs) were observed with the UVCS following slow (~180 km s^{-1}; *Ciaravella et al.* [2002]) and very fast (≥ 1800 km s^{-1}; *Ko et al.* [2003]; *Lin et al.* [2005]) CMEs. Those features were also interpreted in terms of reconnecting current sheets.

Several considerations complicate the above picture of field-line disconnection in a large-scale current sheet. In the simple 2-dimensional view disconnection leads to interplanetary magnetic fields completely unattached to the corona, for which solar wind signatures are rarely, if ever, seen. *Crooker et al.* [2002] have proposed that an interchange reconnection between open coronal fields and closed CME fields, shown in Figure 10, will prevent the addition of new magnetic flux to the interplanetary medium from CMEs. The product will be small closed coronal loops and large open CME fields. Note that disconnection in this 3-dimensional version may still act to form the CME flux rope itself and underlying arcade [*Dere et al.*, 1999], but eventually the flux rope itself must reconnect to prevent an interplanetary magnetic-flux buildup. One question is whether we have any observational evidence of this interchange reconnection, in coronagraph, EUV, soft X-ray, or radio images. We should expect to find interchange reconnection signatures at the peripheries, rather than the centers, of the CME source regions where reconnection with ambient open coronal magnetic fields can occur. Supposing that such reconnection does occur, we are left with two other problems. The first is that the interchange reconnection must occur at only one leg of the CME to produce a resulting flux tube or rope open at only one end [*Crooker et al.*, 2002], which seems very unlikely. The second is that we have seen interplanetary

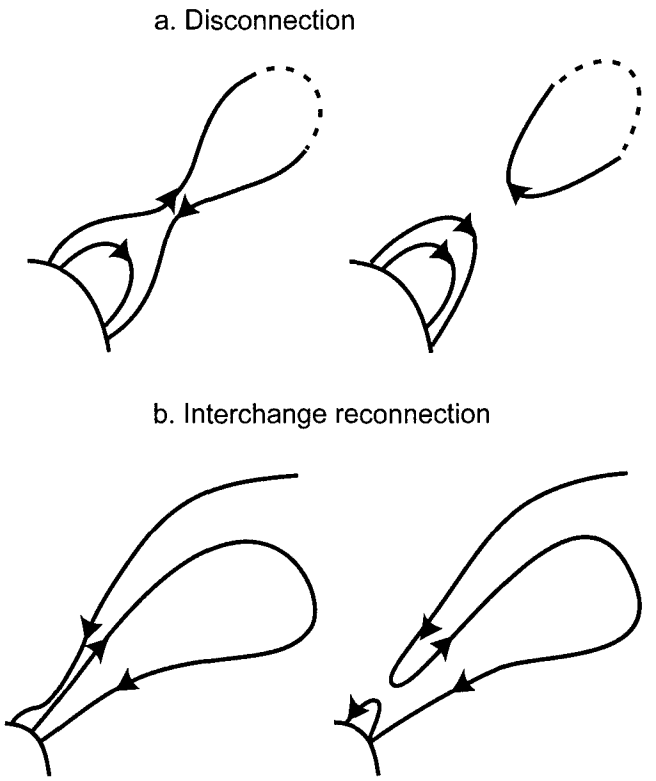

Figure 10. Schematic of the interchange reconnection proposed for the primary method of disconnecting CMEs from the Sun. This reconnection would occur near the periphery of CMEs, away from the central post-eruptive arcade shown in Figure 9. From *Crooker et al.* [2002].

CMEs in which the interior parts of the flux rope are magnetically open and the outer parts are closed, as interpreted from heat-flux electron measurements [*Larson et al.*, 1997]. Those flux-rope open fields would appear to result from a very unlikely reconnection with ambient fields of the same polarity as the flux rope itself if we accept the common interpretation of flux rope geometry [*Burlaga*, 1995]. It remains to find the solar signatures of magnetic reconnection that convert the closed CME fields to open fields and then to understand how that reconnection leads to the complex combinations of open and closed fields observed in interplanetary CMEs.

Coronal reconnection may cause the coronal inflows observed in the LASCO C2 coronagraph [*Sheeley et al.*, 2001; *Sheeley and Wang*, 2001, 2002]. The faint blobs may be described as falling curtains, sinking columns, or inflowing/outflowing pairs [*Simnett*, 2004] with speeds generally < 100 km s^{-1}. The blobs are confined to heights below 5.5 $R_\odot$ and track sector boundaries where oppositely directed fields can reconnect [*Sheeley and Wang*, 2002]. Perhaps surprising is that inflows are not well associated with CMEs [*Sheeley et al.*, 2001], even though the observed inflow rates can reach 30 per day. Are these inflows showing us the characteristic temporal and spatial scales of coronal magnetic reconnection? Why are they not more commonly observed in the aftermath of CMEs? If they represent reconnections between open fields, then why do we not see the interplanetary signatures of disconnected fields?

4.3. Coronal Holes (CHs)and CMEs

CHs are long-lived open-field regions clearly discerned in soft X-ray, He I 10830 Å, and some EUV images. A long-standing question is whether the open fields of CHs may somehow initiate or enhance CMEs from surrounding regions of closed fields. A survey of interplanetary disturbances detected by radio scintillations by *Hewish and Bravo* [1986] showed that all corotating and transient interplanetary shocks originated in CHs. In particular, their transient events, the erupting streams manifested as CMEs, originated in mid-latitude CHs. However, *Harrison* [1990] surveyed 95 CMEs observed on SMM and concluded that CMEs were associated with active regions and not with CHs. Based on another survey showing that CMEs producing interplanetary shocks were associated with CHs, *Bravo* [1995] offered the following scenario. Newly emerging magnetic flux reconnects with opposite polarity fields of an adjacent coronal helmet streamer, producing a CME from the overlying streamer. The area of a CH adjacent to the active region expands, causing the magnetic expansion factor of the CH to decrease with a transient increase in the solar wind flow speed. Other studies by *Bravo and Rivera* [1994] and by *Gonzalez et al.* [1996] showed that the solar sources of the most intense interplanetary disturbances and geomagnetic storms were active regions near low-latitude CHs. *Gonzalez et al.* [1996] called these sources of active regions (with flares and/or filament eruptions) occurring close to the streamer belt and to growing low-latitude CHs CHARCS (for CH-Active Region-Current Sheet). *Bravo et al.* [1998] found a solar-cycle correlation between active regions near CHs and intense geomagnetic storms, further strengthening the connection of shock-producing CMEs and CHARCS.

A more direct connection between CMEs and CHs was found in Yohkoh SXT images by *Bhatnagar* [1996], who studied 15 large post-eruptive X-ray loop arcades outside active regions. These events, called X-ray blowouts, were not associated with observed chromospheric activity, but all were located at or near the boundaries of CHs. *Bhatnagar* [1996] proposed for the blowouts an interaction between the open CH fields and opposite polarity fields of adjacent closed field regions. *Webb et al.* [1978] had earlier found a significant, but not strong, tendency for Skylab X-ray arcades outside active regions to occur over neutral lines forming the borders of CHs. *Lewis and Simnett* [2000] performed a statistical study of CME source locations near solar minimum (1996-97) and found the centroid of CME sources to be located about 45° west of an active region complex, in the vicinity of a polar CH extension to low latitudes. A more extreme example is that of an erupting filament and CME on 28 December 1999 observed with Yohkoh/SXT, EIT, and LASCO by *Chertok et al.* [2002], who interpreted the source to lie inside a large transequatorial CH.

These observations suggest that low-latitude CHs may be important for at least some CMEs. The adjacent open fields of the CHs may interact with closed fields of the CMEs either by magnetic reconnection or by deflecting the courses of the CMEs away from the CHs. A significant equatorward deflection of CME trajectories, attributed to polar coronal holes is observed around solar minimum [*Cremades and Bothmer*, 2004]. However, we do not yet have a good observational understanding of CME source regions and CHs. Among the questions to answer are the following. How often are CME source regions adjacent to CHs? If so, what are the CH characteristics in terms of their sizes and growth rates? Are more energetic CMEs more likely to lie adjacent to CHs? What is the effect of CHs on CMEs - reconnection with closed field regions or deflections or modifications of CME trajectories?

5. SUMMARY

We now have white-light CME observations over several solar cycles from coronagraphs of increasing capabilities in terms of dynamic range, cadence, and field of view. The $> 10{,}000$ CMEs thus far observed have been statistically

analyzed for their average and median properties and the variations of the properties over the solar cycle. The coronagraph observations have been supplemented with ground-based coronameter and Hα observations, as well as EUV, X-ray, and radio observations that have allowed us to study details of the structures, early dynamics and source regions of CMEs. However, with this abundance of white light observations there is still a real dearth of spectral line observations needed to assess temperature, velocity, and density distributions that can tell us about the spatial and temporal dynamics of CMEs.

As is the case with solar flares, our increasing wealth of observations has been accompanied by a slow progress in understanding the fundamental questions posed by CMEs. We still have difficulty determining the exact source regions of CMEs even when the sources are near central meridian and well observed in EUV and X-rays. The CME magnetic field geometries and topologies are unclear, and the way in which the expelled magnetic fields of CMEs reconnect to convert themselves to open magnetic fields has yet to be defined.

Acknowledgments. I thank the organizers for my travel support and for arranging a superb Chapman Conference.

REFERENCES

Akmal, A., *et al.*, SOHO observations of a coronal mass ejection, *Astrophys. J.*, 553, 922, 2001.

Aoki, S.I., S. Yashiro, and K. Shibata, The log-normal distributions of coronal mass ejection-related solar flares and the flare/CME model of gamma-ray bursts, *Proc. 28th Int. Cosmic Ray Conf.*, 5, 2729, 2003.

Athay, R.G., B.C. Low, and B. Rompolt, Characteristics of the expansion associated with eruptive prominences, *Sol. Phys.*, 110, 359, 1987.

Bhatnagar, A., Solar mass ejections and coronal holes, *Astrophys. Space Sci.*, 243, 105, 1996.

Bogdan, T., P.A. Gilman, I. Lerche, and R. Howard, Distribution of sunspot umbral areas: 1917-1982, *Astrophys. J.*, 327, 451, 1988.

Bravo, S., A solar scenario for the associated occurrence of flares, eruptive prominences, coronal mass ejections, coronal holes, and interplanetary shocks, *Sol. Phys.*, 161, 57, 1995.

Bravo, S., and A.L. Rivera. The solar causes of major geomagnetic storms, *Ann. Geophys.*, 12, 113, 1994.

Bravo, S., J.A.L. Cruz-Abayro, and D. Rojas, The spatial relationship between active regions and coronal holes and the occurrence of intense geomagnetic storms throughout the solar activity cycle, *Ann. Geophys.*, 16, 49, 1998.

Brueckner, G.E., *et al.*, The Large Angle Spectroscopic Coronagraph (LASCO), *Sol. Phys.*, 162, 357, 1995.

Burkepile, J.T., A.J. Hundhausen, A.L. Stanger, O.C. St. Cyr, and J.A. Seiden, Role of projection effects on solar coronal mass ejection properties: 1. A study of CMEs associated with limb activity, *J. Geophys. Res.*, 109, A03103, doi:10.1029/2003JA010149, 2004.

Burlaga, L.F., *Interplanetary Dynamics,* p.89, Oxford University Press, New York, 1995.

Campbell, W.H., *Introduction to Geomagnetic Fields,* p.293, Cambridge U. Press, Cambridge, 2003.

Chané, E., C. Jacobs, B. Van der Holst, S. Poedts, and D. Kimpe, On the effect of the initial magnetic polarity and of the background wind on the evolution of CME shocks, *Astron. Astrophys.*, 432, 331, 2005.

Chen, J., and J. Krall, Acceleration of coronal mass ejections, *J. Geophys. Res.*, 108(11), 1410, doi:10.1029/2003JA009849, 2003.

Chertok, I.M., E.I. Mogilevsky, V.N. Obridko, N.S. Shilova, and H.S. Hudson, Solar disappearing filament inside a coronal hole, *Astrophys. J.*, 567, 1225, 2002.

Ciaravella, A., *et al.*, Solar and Heliospheric Observatory observations of a helical coronal mass ejection, *Astrophys. J.*, 529, 575, 2000.

Ciaravella, A., J.C. Raymond, J. Li, P. Reiser, L.D. Gardner, Y.-K. Ko, and S. Fineschi, Elemental abundances and post-coronal mass ejection current sheet in a very hot active region, *Astrophys. J.*, 575, 1116, 2002.

Ciaravella, A., J.C. Raymond, A. van Ballegooijen, L. Strachan, A. Vourlidas, J. Li, J. Chen, and A. Panasyuk, Physical parameters of the 2000 February 11 coronal mass ejection: ultraviolet spectra versus white-light images, *Astrophys. J.*, 597, 1118, 2003.

Cremades, H., and V. Bothmer, On the three-dimensional configuration of coronal mass ejections, *Astron. Astrophys.*, 422, 307, 2004.

Crooker, N.U., J.T. Gosling, and S.W. Kahler, Reducing heliospheric magnetic flux from coronal mass ejections without disconnection, *J. Geophys. Res.*, 107(A2), doi:10.1029/2001JA000236, 2002.

Dere, K.P., G.E. Brueckner, R.A. Howard, D.J. Michels, and J.P. Delaboudiniere, LASCO and EIT observations of helical structure in coronal mass ejections, *Astrophys. J.*, 516, 465, 1999.

Dere, K.P., D. Wang, and R. Howard, Three-dimensional structure of coronal mass ejections from LASCO polarization measurements, *Astrophys. J.*, 620, L119, 2005.

Dobrzycka, D., J.C. Raymond, D.A. Biesecker, J. Li, and A. Ciaravella, Ultraviolet spectroscopy of narrow coronal mass ejections, *Astrophys. J.*, 588, 586, 2003.

Feynman, J., and A. Ruzmaikin, A high-speed erupting-prominence CME: a bridge between types, *Sol. Phys.*, 219, 301, 2004.

Gallagher, P.T., G.R. Lawrence, and B.R. Dennis, Rapid acceleration of a coronal mass ejection in the low corona and implications for propagation, *Astrophys. J.*, 588, L53, 2003.

Gilbert, H.R., E.C. Serex, T.E. Holzer, R.M. MacQueen, and P.S. McIntosh, Narrow coronal mass ejections, *Astrophys. J.*, 550, 1093, 2001.

Gonzalez, W.D., B.T. Tsurutani, P.S. McIntosh, and A.L. Clua de Gonzalez, Coronal hole-active region-current sheet (CHARCS) association with intense interplanetary and geomagnetic activity, *Geophys. Res. Lett.*, 23, 2577, 1996.

Gopalswamy, N., A global picture of CMEs in the inner heliosphere, in *The Sun and the Heliosphere as an Integrated system,* edited by G. Poletto and S. Suess, ASSL Kluwer, Dordrecht, 2004.

Gopalswamy, N., A. Lara, S. Yashiro, S. Nunes, and R.A. Howard, Coronal mass ejection activity during solar cycle 23, in *Proc. Solar variability as an input to the Earth's environment. International Solar Cycle Studies (ISCS) Symposium,* edited by A. Wilson, p.403, ESA SP-535, 2003.

Gosling, J.T., Large-scale inhomogeneities in the solar wind of solar origin, *Rev. Geophys.*, 13, 1053, 1975.

Gosling, J.T., E. Hildner, R.M. MacQueen, R.H. Munro, A.I. Poland, and C.L. Ross, The speeds of coronal mass ejection events, *Sol. Phys.*, 48, 389, 1976.

Harrison, R.A., The source regions of solar coronal mass ejections, *Sol. Phys.*, 126, 185, 1990.

Hewish, A., and S. Bravo, The sources of large-scale heliospheric disturbances, *Sol. Phys.*, 106, 185, 1986.

Hundhausen, A., Coronal mass ejections, in *The Many Faces of the Sun: a summary of the results from NASA's Solar Maximum Mission,* edited by K.T. Strong, et al., p.143, Springer, New York, 1999.

Illing, R.M.E., and R.G. Athay, Physical conditions in eruptive prominences at several solar radii, *Sol. Phys.*, 105, 173, 1986.

Jackson, B.V., and D.F. Webb, The masses of CMEs measured in the inner heliosphere, in *Proc. Third SOHO Wkshp,* p. 233, ESA SP-373, 1994.

Jing, J., J. Qiu, J. Lin, M. Qu, Y. Xu, and H. Wang, Magnetic reconnection rate and flux-rope acceleration of two-ribbon flares, *Astrophys. J.*, 620, 1085, 2005.

Kahler, S.W., N.R. Sheeley, Jr., and M. Liggett, Coronal mass ejections and associated X-ray flare durations, *Astrophys. J.*, 344, 1026, 1989.

Kahler, S.W., D.V. Reames, and N.R. Sheeley, Jr., Coronal mass ejections associated with impulsive solar energetic particle events, *Astrophys. J.*, 562, 558, 2001.

Kahler, S.W., and D.V. Reames, Solar energetic particle production by coronal mass ejection-driven shocks in solar fast-wind regions, *Astrophys. J.*, 584, 1063, 2003.

Ko, Y.-K., J.C. Raymond, J. Lin, G. Lawrence, J. Li, and A. Fludra, Dynamical and physical properties of a post-coronal mass ejection current sheet, *Astrophys. J.*, 594, 1068, 2003.

Larson, D.E., et al., Tracing the topology of the October 18-20, 1995, magnetic cloud with ~0.1-10^2 keV electrons, *Geophys. Res. Lett.*, 24, 1911, 1997.

Lewis, D.J., and G.M. Simnett, The occurrence of coronal mass ejection at solar minimum and their association with surface activity, *Sol. Phys.*, 191, 185, 2000.

Lin, J., CME-flare association deduced from catastrophic model of CMEs, *Sol. Phys.*, 219, 169, 2004.

Lin, J., J.C. Raymond, and A.A. van Ballegooijen, The role of magnetic reconnection in the observable features of solar eruptions, *Astrophys. J.*, 602, 422, 2004.

Lin, J., Y.-K. Ko, L. Sui, J.C. Raymond, G.A. Stenborg, Y. Jiang, S. Zhao, and S. Mancuso, Direct observations of the magnetic reconnection site of an eruption on 2003 November 18, *Astrophys. J.*, it 622, 1251, 2005.

Liu, W., X.P. Zhao, S.T. Wu, and P. Scherrer, Effects of magnetic topology on CME kinematic properties, in *Proc. Solar variability as an input to the Earth's environment. International Solar Cycle Studies (ISCS) Symposium,* edited by A. Wilson, p.459, ESA SP-535, 2003.

Low, B.C., and M. Zhang, The hydromagnetic origin of the two dynamical types of solar coronal mass ejections, *Astrophys. J.*, 564, L53, 2002.

MacQueen, R.M., A. Csoeke-Poeckh, E. Hildner, L. House, R. Reynolds, A. Stanger, H. Tepoel, and W. Wagner, The high altitude observatory coronagraph/polarimeter on the Solar Maximum Mission, *Sol. Phys.*, 65, 91, 1980.

MacQueen, R.M., and R.R. Fisher, The kinematics of solar inner coronal transients, *Sol. Phys.*, 89, 89, 1983.

Maricic, D., B. Vršnak, A.L. Stanger, D. Rosa, and D. Hrzina, Initiation and development of two coronal mass ejections, in *Proc. Solar variability as an input to the Earth's environment. International Solar Cycle Studies (ISCS) Symposium*, edited by A. Wilson, p.441, ESA SP-535, 2003.

Maričić, D., B. Vršnak, A.L. Stanger, and A. Veronig, Coronal mass ejection of 15 May 2001: I. evolution of morphological features of the eruption, *Sol. Phys.*, 225, 337, 2004.

McAllister, A.H., D.H. McKay, and S.F. Martin, The skew of high-latitude X-ray arcades in the declining phase of cycle 22, *Sol. Phys.*, 211, 155, 2002.

McKenzie, D.E., Supra-arcade downflows in long-duration solar flare events, *Sol. Phys.*, 195, 381, 2000.

Michalek, G., and J. Mazur, Properties of coronal mass ejections, in *Proc. 10th Eur. Solar Phys. Mtg, Prague, 1*, edited by A. Wilson, p.181, ESA SP-506, 2002.

Michalek, G., N. Gopalswamy, and S. Yashiro, A new method for estimating widths, velocities, and source location of halo coronal mass ejections, *Astrophys. J.*, 584, 472, 2003.

Moon, Y.-J., G.S. Choe, H. Wang, Y.D. Park, N. Gopalswamy, G. Yang, and S. Yashiro, A statistical study of two classes of coronal mass ejections, *Astrophys. J.*, 581, 694, 2002.

Moon, Y.-J., K.S. Cho, Z. Smith, C.D. Fry, M. Dryer, and Y.D. Park, Flare-associated coronal mass ejections with large accelerations, *Astrophys. J.*, 615, 1011, 2004.

Moran, T.G., and J.M. Davila, Three-dimensional polarimetric imaging of coronal mass ejections, *Sci.*, 305, 66, 2004.

Pick, M., P. Démoulin, S. Krucker, O. Malandraki, and D. Maia, Radio and X-ray signatures of magnetic reconnection behind an ejected flux rope, *Astrophys. J.*, 625, 1019, 2005.

Plunkett, S.P., *et al.*, Simultaneous SOHO and ground-based observations of a large eruptive prominence and coronal mass ejection, *Sol. Phys.*, 194, 371, 2000.

Raymond, J.C., Spectroscopic diagnostics of CME material, in *Proceedings of the SOHO 11 Symposium on From Solar Min to Max: Half a Solar Cycle with SOHO*, edited by A. Wilson, p.421, ESA SP-508, 2002.

Raymond, J.C., A. Ciaravella, D. Dobrzycka, L. Strachan, Y.-K. Ko, M. Uzzo, and N.-E. Raouafi, Far-ultraviolet spectra of fast coronal mass ejections associated with X-class flares, *Astrophys. J.*, 597, 1106, 2003.

Reames, D.V., Magnetic topology of impulsive and gradual solar energetic particle events, *Astrophys. J.*, 571, L63, 2002.

Robbrecht, E., and D. Berghmans, Automated recognition of coronal mass ejections (CMEs) in near-real-time data, *Astron. Astrophys.*, 425, 1097, 2004.

Shanmugaraju, A., Y.-J. Moon, M. Dryer, and S. Umapathy, On the kinematic evolution of flare-associated CMEs, *Sol. Phys.*, 215, 185, 2003.

Sheeley, N.R., Jr., D.J. Michels, R.A. Howard, and M.J. Koomen, Initial observations with the Solwind coronagraph, *Astrophys. J.*, 237, L99, 1980.

Sheeley, N.R., Jr., J.H. Walters, Y.-M. Wang, and R.A. Howard, Continuous tracking of coronal outflows: Two kinds of coronal mass ejections, *J. Geophys. Res.*, 104, 24739, 1999.

Sheeley, N.R., Jr., T.N. Knudson, and Y.-M. Wang, Coronal inflows and the Sun's nonaxisymmetric open flux, *Astrophys. J.*, 546, L131, 2001.

Sheeley, N.R., Jr., and Y.-M. Wang, Coronal inflows and sector magnetism, *Astrophys. J.*, 562, L107, 2001.

Sheeley, N.R., Jr., and Y.-M. Wang, Characteristics of coronal inflows, *Astrophys. J.*, 579, 874, 2002.

Shibata, K., Evidence of magnetic reconnection in solar flares and a unified model of flares, *Astrophys. Space Sci.*, 264, 129, 1999.

Shimojo, M., and K. Shibata, Physical parameters of solar X-ray jets, *Astrophys. J.*, 542, 1100, 2000.

Simnett, G.M., The relationship between prominence eruptions and coronal mass ejections, *J. Atmos. Terr. Phys.*, 62, 1479, 2000.

Simnett, G.M., Evidence for magnetic reconnection in the high corona, *Astron. Astrophys.*, 416, 759, 2004.

Simnett, G.M., *et al.*, LASCO observations of disconnected magnetic structures out to beyond 28 solar radii during coronal mass ejections, *Sol. Phys.*, 175, 685, 1997.

St. Cyr, O.C., J.T. Burkepile, A.J. Hundhausen, and A.R. Lecinski, A comparison of ground-based and spacecraft observations of coronal mass ejections from 1980-1989, *J. Geophys. Res.*, 104, 12493, 1999.

St. Cyr, O.C., *et al.*, Properties of coronal mass ejections: SOHO LASCO observations from January 1996 to June 1998, *J. Geophys. Res.*, 105(A8), 18169, 2000.

St. Cyr, O.C., *et al.*, The last word: the definition of halo coronal mass ejections, *EOS*, 86(30), 281, 2005.

Stockton-Chalk, A., The limit of non-radial expansion of coronal mass ejections, in *Proc. SOLSPA: The second solar cycle and space weather euroconference, ESA* SP-477, 277, 2002.

Svestka, Z., On the varieties of solar flares, in *The lower atmosphere of solar flares; Proc. Solar Maximum Mission Symp.*, edited by D.F. Neidig, p.332, National Solar Observatory, 1986.

Tripathi, D., V. Bothmer, and H. Cremades, The basic characteristics of EUV post-eruptive arcades and their role as tracers of coronal mass ejection source regions, *Astron. Astrophys.*, 422, 337, 2004.

Vourlidas, A., D. Buzasi, R.A. Howard, and E. Esfandiari, Mass and energy properties of LASCO CMEs, in *Proc. 10th Eur. Solar Phys. Mtg, Prague, 1*, edited by A. Wilson, p.91, ESA SP-506, 2002.

Vourlidas, A., private comm., 2004.

Vršnak, B., D. Ruždjak, D. Sudar, and N. Gopalswamy, Kinematics of coronal mass ejections between 2 and 30 solar radii: What can be learned about forces governing the eruption?, *Astron. Astrophys.*, 423, 717, 2004.

Vršnak, B., D. Sudar, and D. Ruždjak, The CME-flare relationship: Are there really two types of CMEs?, *Astron. Astrophys.*, 435, 1149, 2005.

Wang, Y.-M., and N.R. Sheeley, Jr., Observations of core fallback during coronal mass ejections, *Astrophys. J.*, 567, 1211, 2002a.

Wang, Y.-M., and N.R. Sheeley, Jr., Coronal white-light jets near sunspot maximum, *Astrophys. J.*, 575, 542, 2002b.

Wang, Y.-M., and N.R. Sheeley, Jr., Sunspot activity and the long-term variation of the Sun's open magnetic flux, *J. Geophys. Res.*, 107, 1302, doi:10.1029/2001JA000500, 2002c.

Webb, D.F., P.S. McIntosh, J.T. Nolte, and C.V. Solodyna, Evidence linking coronal transients to the evolution of coronal holes, *Sol. Phys.*, 58, 389, 1978.

Webb, D.F., and E.W. Cliver, Evidence for magnetic disconnection of mass ejections in the corona, *J. Geophys. Res.*, (A4), 5853, 1995.

Webb, D.F., J. Burkepile, T.G. Forbes, and P. Riley, Observational evidence of new current sheets trailing coronal mass ejections, *J. Geophys. Res.*, 108, 1440, doi:10.1029/2003JA009923, 2003.

Xie, H., L. Ofman, and G. Lawrence, Cone model for halo CMEs: application to space weather forecasting, *J. Geophys. Res.*, 109, A03109, doi:10.1029/2003JA010226, 2004.

Yashiro, S., N. Gopalswamy, G. Michalek, and R.A. Howard, Properties of narrow coronal mass ejections observed with LASCO, *Adv. Space Res.*, 32, 2631, 2003.

Yashiro, S., N. Gopalswamy, G. Michalek, O.C. St.Cyr, S.P. Plunkett, N.B. Rich, and R.A. Howard, A catalog of white light coronal mass ejections observed by the SOHO spacecraft, *J. Geophys. Res.*, 109, A07105, doi:10.1029/2003JA010282, 2004.

Yurchyshyn, V., S. Yashiro, V. Abramenko, H. Wang, and N. Gopalswamy, Statistical distributions of speeds of coronal mass ejections, *Astrophys. J.*, 619, 599, 2005.

Zhang, J., K.P. Dere, R.A. Howard, M.R. Kundu, and S.M. White, On the temporal relationship between coronal mass ejections and flares, *Astrophys. J.*, 559, 452, 2001.

Zhang, J., K.P. Dere, R.A. Howard, and A. Vourlidas, A study of the kinematic evolution of coronal mass ejections, *Astrophys. J.*, 604, 420, 2004.

Zhang, M., and L. Golub, The dynamical morphologies of flares associated with the two types of solar coronal mass ejections, *Astrophys. J.*, 595, 1251, 2003.

Zhang, M., L. Golub, E. DeLuca, and J. Burkepile, The timing of flares associated with the two dynamical types of solar coronal mass ejections, *Astrophys. J.*, 574, L97, 2002.

Zhao, X.P., S.P. Plunkett, and W. Liu, Determination of geometrical and kinematical properties of halo coronal mass ejections using the cone model, *J. Geophys. Res.*, 107(A8), 1223, doi:10.1029/2001JA009143, 2002.

S. Kahler, AFRL/VSBXS, 29 Randolph Rd., Hanscom AFB, MA 01731. (Stephen.kahler@hanscom.af.mil)